Optical tomographic imaging of small animals

Andreas H Hielscher

Diffuse optical tomography is emerging as a viable new biomedical imaging modality. Using visible and near-infrared light this technique can probe the absorption and scattering properties of biological tissues. The main applications are currently in brain, breast, limb and joint imaging; however, optical tomographic imaging of small animals is attracting increasing attention. This interest is fuelled by recent advances in the transgenic manipulation of small animals that has led to many models of human disease. In addition, an ever increasing number of optically reactive biochemical markers has become available, which allow diseases to be detected at the molecular level long before macroscopic symptoms appear. The past three years have seen an array of novel technological developments that have led to the first optical tomographic studies of small animals in the areas of cerebral ischemia and cancer.

Addresses
Departments of Biomedical Engineering & Radiology, Columbia University, 500 West 120th Street, MC8904, ET351 Mudd Building, New York, NY 10027, USA

Corresponding author: Hielscher, Andreas H (ahh2004@columbia.edu)

Abbreviations

BLT	bioluminescence tomography
DOT	diffuse optical tomography
DYNOT	dynamic near-infrared optical tomography
FD	frequency domain
MOBIIR	model-based iterative image reconstruction
MRI	magnetic resonance imaging
PET	positron emission tomography
SPECT	single-photon emission computed tomography
SSD	steady-state domain
TD	time domain

Introduction

Over the past decade considerable progress has been made towards the development of a novel tomographic imaging modality that uses light in the wavelength range $500\,\text{nm} < \lambda < 900\,\text{nm}$ to probe biomedical tissues [1–3]. Besides diffuse optical tomography (DOT), various other names have been used to describe this technology, such as optical diffuse tomography, photon migration tomography or just optical tomography. DOT has so far been mainly applied to breast cancer diagnostics [4,5], joint imaging [6,7] and blood oximetry in human muscle and brain tissue [8–10].

More recently, the first studies and systems to focus on the optical tomographic imaging of small animals have emerged [11••,12••,13•,14,15••]. The interest in small-animal imaging is motivated by progress in the transgenic manipulation of small animals, which has allowed models to be developed for a variety of human diseases. Using these models it is possible to link specific genes, proteins and enzymes to molecular and cellular processes that underlie various disorders. In addition, the advent of novel biochemical markers that are sensitive to molecular processes, defect genes and cell receptors, makes it possible for the first time to detect diseases on a molecular level long before actual phenotypical symptoms appear [16,17].

Employing small-animal imaging systems it has become possible to perform noninvasive assays for monitoring the progression of diseases and biological processes. Small-animal optical tomography has several advantages over other, more traditional, imaging modalities. For example, optical markers emit low-energy near-infrared photons that are less harmful than more energetic γ-rays emitted from radioactive markers (used in single-photon emission computed tomography [SPECT] and positron emission tomography [PET], for instance) [18]. This simplifies synthesis procedures and experimental designs and will be of particular importance for future applications in humans. Furthermore, optical methods typically offer higher sensitivity (as compared with magnetic resonance imaging [MRI] and SPECT) and are relatively inexpensive (as compared with PET, SPECT and MRI).

In this paper we will review the underlying principles of optical tomographic imaging, as applied to studies involving small animals. We will describe the basic contrast mechanism involved in imaging of both endogenous and exogenous contrast agents, and discuss common instrumentation and image reconstruction strategies. Furthermore, we will provide an overview of the most recently published small-animal imaging studies in the areas of blood oximetry, and fluorescence- and bioluminescence-enhanced imaging.

Imaging with endogenous contrast
The basis of contrast

In DOT, low-energy electromagnetic radiation (∼1 to 2.5 eV) is delivered to one or more locations on the surface

of the body part under investigation and transmitted and/ or back-reflected light intensities are measured at distances up to 10 cm. Unlike medical X-rays (photon energy $\sim$5 to 150 keV), which pass through the body almost unscattered, photons used for optical tomography undergo multiple scattering before they leave the medium. The scattering properties of the tissue are described by the spatially varying scattering coefficient, $\mu_s(r)$. Also commonly used is the reduced or transport scattering coefficient $\mu_s' = (1-g)\mu_s$, where $g \in [-1,1]$ is a parameter that describes the anisotropic scattering properties of a tissue [19]. Differences in the refractive index between intracellular and extracellular fluids, and between various subcellular components such as mitochondria or nuclei, as well as varying tissue densities give rise to differences in scattering coefficients and g factors [20,21].

Besides being scattered, near-infrared light can also be absorbed by a multitude of chromophores inside the tissue; for example, endogenous chromophores include hemoglobin, cytochromes, flavins and porphyrins. Of special interest for tissue oximetry are oxyhemoglobin and deoxyhemoglobin and derived parameters such as oxygen saturation [13•]. Differences in chromophore content and concentration lead to different absorption coefficients $\mu_a(r)$.

Optical tomographic imaging modalities

In general, optical imaging systems can be divided into three different categories: time-domain (TD) systems, frequency-domain (FD) devices, and steady-state domain (SSD) instrumentation, often also referred to as continuous wave systems [22]. When TD methods are employed, a short laser pulse (typically of duration less than 1×10^{-10} seconds) is injected into the tissue. Travelling through the tissue this pulse broadens and its peak intensity becomes smaller (Figure 1a). The extent of these effects is influenced by the optical properties and the distances travelled inside the tissue before being recorded. For example, the time at which the maximum of the response function is reached is indicative of μ_s. The decreasing slope of the response curve yields information about μ_a [23]. Time-resolved systems for small-animal imaging are still in their nascent state. The smaller tissue volumes encountered in small animals require especially high temporal resolutions, which poses added technological challenges [24•].

Instead of using a short light pulse, FD systems use sinusoidally amplitude-modulated light sources [25]. The modulation frequency is typically between 100–1000 MHz [26]. The measured parameters are the phase shift, Φ, and the demodulation, $M = (AC_o/DC_o)/(AC_i/DC_i)$, of the light transmitted through the tissue relative to the incident light (Figure 1b). Measuring Φ and M for all frequencies amounts to performing the Fourier transform of the TD data. FD systems that focus on small-animal

Figure 1
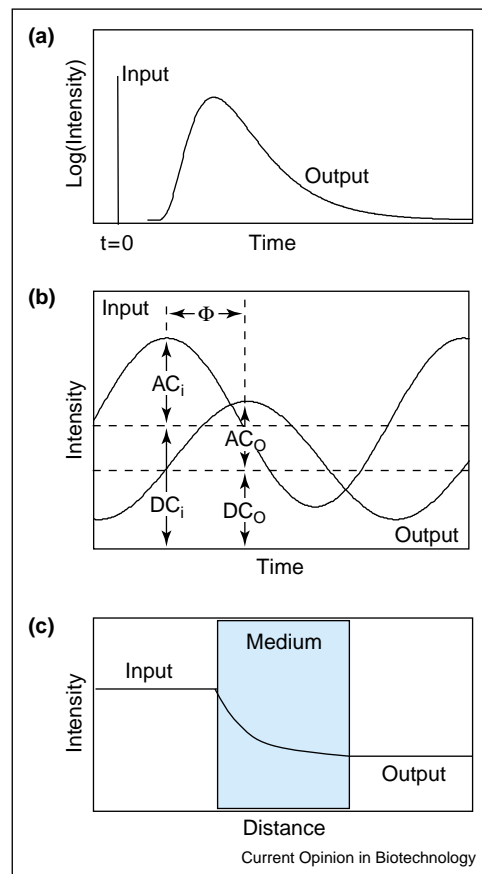
Different modes of data acquisition for optical tomography. **(a)** Time domain (TD), **(b)** frequency domain (FD) and **(c)** steady-state domain (SSD; also commonly referred to as continuous wave domain).

imaging have been developed by Yodh and colleagues [27,28•] and by Thompson and Sevick-Muraca [29].

Originally thought to be of limited use, SSD systems have made a comeback in recent years and are now among the most widely used in clinical settings as well as for small-animal imaging. In SSD systems the light source continuously emits light into the tissue and the transmitted light intensities are measured (Figure 1c). An example of such a system is the dynamic near-infrared optical tomography (DYNOT) instrument, recently developed by Schmitz et al. [30•]. In this instrument, two wavelengths between 700 nm and 850 nm are provide by two laser diodes, the light of which is sequentially coupled into 32 different fiber bundles. These optical fibers deliver the light to various positions on the surface of the tissue and are also used to collect transmitted light intensities. A full tomographic dataset (two wavelength at $32 \times 32 = 992$ source-detector configuration) can be obtained in approximately 0.5 s, leading to a data acquisition rate of

$2 \times 992/0.5 = 3968$ measurements per second. This is the fastest data acquisition rate (measurement points per second) of all currently available optical tomography instruments. Similar instruments have been developed by Siegel *et al.* [31,32•] and Cheung *et al.* [27].

Image reconstruction algorithms

The majority of currently available image reconstruction codes can be classified as model-based iterative image reconstruction (MOBIIR) algorithms [33,34]. These iterative reconstruction schemes usually contain three major components: a forward model, an analysis scheme, and an updating scheme (see Figure 2). Variations between different codes in the updating scheme usually affect the convergence rate of the algorithm [35], whereas differences in the objective function [36–38] and forward model affect the accuracy of the code. The most accurate forward model is given by the equation of radioactive transfer [39,40••,41••,42]. However, if $\mu_s >> \mu_a$, which is often the case in practical situations, the simpler diffusion equation can be used. It has been argued that because of the small geometries encountered in small-animal imaging, diffusion-equation-based codes should not be applied because the inherent approximations are no longer valid [43••,44•]. Nevertheless, most of the current

small-animal imaging systems use the diffusion equation in the reconstruction process, and what type of algorithm will perform best under the given circumstance is still to be determined. There is some indication that when relative changes rather than absolute values of optical properties are sought, the accuracy of the forward model plays less of a role [45,46•].

Overall the image reconstruction problem in optical tomography is highly ill-posed [34]. This means that different distribution of optical properties inside the tissue can lead to the same measurements observed on the surface of the tissue. To nevertheless obtain reasonable results, some sort of constraints typically have to be imposed on the solution [36–38]. For example it is often assumed that the results are within a certain range of absorption or scattering values or that scattering properties do not change during hemodynamic perturbations.

## Comparison of different systems

The information content and the complexity of hardware and imaging software increases from SSD to FD and TD systems. The obtainable spatial resolution, given the same number of sources and detectors, also increases from SSD to FD to TD systems. However, SSD systems

Figure 2
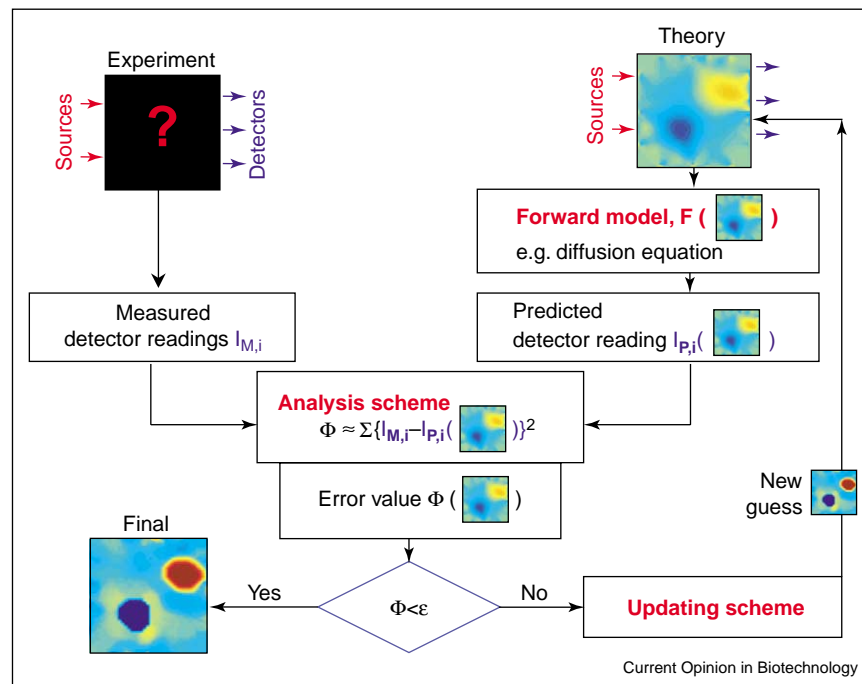
Basic structure of a model-based iterative image reconstruction (MOBIIR) scheme commonly used in DOT. MOBIIR schemes usually contain three major components. The first component is a so-called forward model that provides a prediction of the measurements based on a guess of the system parameters (here the spatial distribution of μ_a and μ_s') and given source positions. The second element, the analysis scheme, compares the predicted data with the measured data, which results in some sort of error function (often also called the objective function or norm). The third part is an updating scheme that provides a new set of system parameters for the forward model, depending on the mismatch between predicted and measured data. With this set of new system parameters a new forward calculation is performed. The set of spatially varying μ_a and μ_s' values for which the objective function is minimized constitutes the final image.

Figure 3
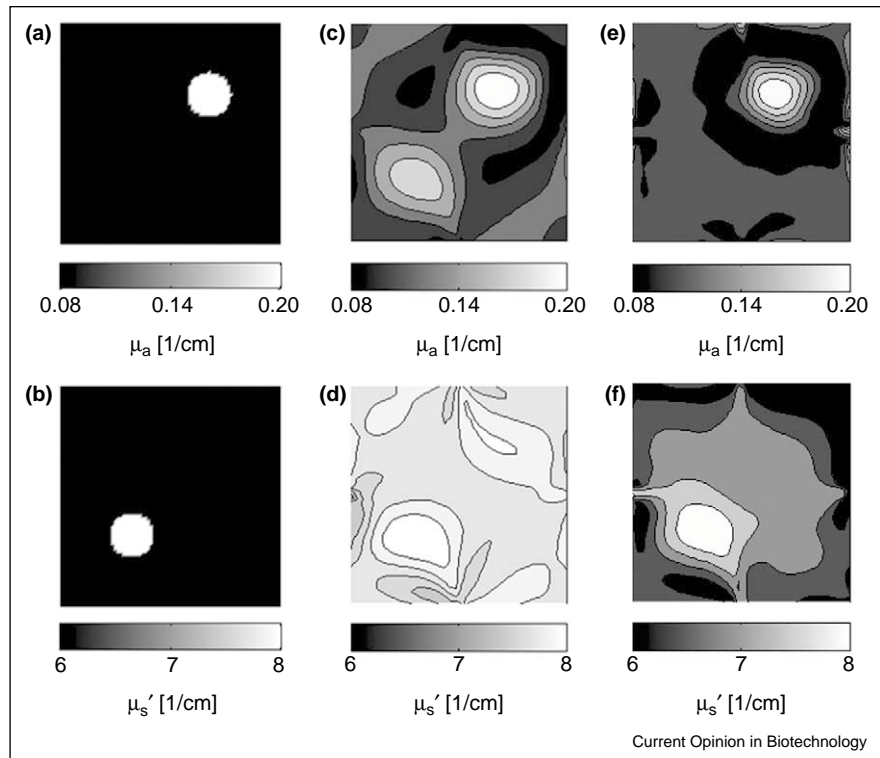
Frequency domain versus steady-state domain image reconstruction. **(a)** Original map of spatial distribution of the absorption coefficient μ_a. **(b)** Original map of spatial distribution of the scattering coefficient μ_s'. **(c,d)** Reconstruction results using SSD data. **(e,f)** Reconstruction results using FD data at a source modulation frequency of $\omega = 200$ MHz. For the reconstructions, data from four source and 16 detectors equally distributed on the circumference of the 2×2 cm square were used. All reconstructions started with an initial guess of a homogenous medium with $\mu_a = 0.12$ cm^{-1} and $\mu_s' = 7.2$ cm^{-1}. The MOBIIR code used for this example is based on the equation of radiative transfer [89]. Clearly visible is the cross-talk between absorption and scattering effects in the images (c) and (d) that were obtained from SSD data ($\omega = 0$ MHz). (e,f) As expected, a much better separation of scattering and absorption effects is obtained when FD data are used.

allow for much faster data acquisition than TD systems. While SSD systems allow for data acquisition rates for one source and one detector of up to 8000, FD system are currently limited to ~10–400 and TD systems to typically less than 1 [30•]. This allows SSD systems to look at fast physiological changes, such as hemodynamic effects in the brain or limbs. TD systems usually take more than 1 min and fast physiological changes cannot be imaged.

Another important aspect in DOT is the ability to distinguish between scattering and absorption effects. As SSD measurements provide less information, in general, it is more difficult to distinguish scattering from absorption effects using SSD-type data than when FD or TD data are used [34••,47,48] (see example in Figure 3). Theoretical studies have shown that SSD imaging is highly ill-posed and does not, in general, allow separation of absorption and scattering effects. However, in practical cases additional constraints can often be introduced, which makes the separation of absorption and scattering possible even with SSD systems [49,50].

Applications

In the past three years, applications of small-animal imaging with endogenous contrast have focused on two areas: blood oximetry, as it relates to cerebral ischemia, and functional imaging [51••]. In these cases, μ_a and μ_s are not the goal of the image reconstruction, but rather the concentration of oxyhemoglobin [HbO$_2$] and deoxyhemoglobin [Hb] and derived parameters such as total hemoglobin concentration [THb] = [HbO$_2$] + [Hb] or blood saturation S = [HbO$_2$]/[THb]. Assuming that the primary influence on μ_a is a linear combination of [HbO$_2$] and [Hb], one arrives at [52,53]:

$$\mu_a^\lambda = \varepsilon_{HbO}^\lambda [HbO] + \varepsilon_{Hb}^\lambda [Hb]$$

By performing tomographic reconstructions of μ_a at two wavelengths, λ_1 and λ_2, one can solve the resulting set of two algebraic equations for the concentrations of [HbO$_2$] and [Hb], respectively. This concept is easily extended to more than two chromophores, by employing n different wavelengths if n chromophores are sought. Recent works

Figure 4
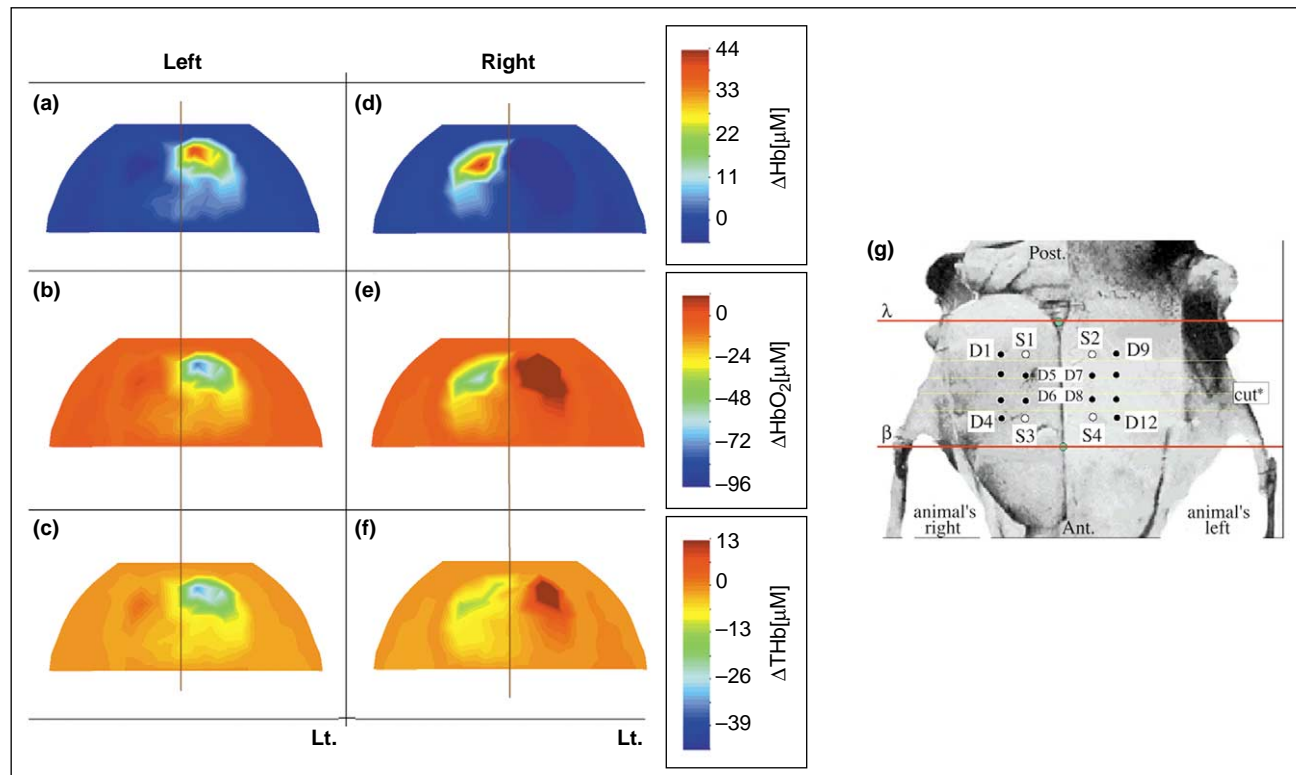
Optical tomographic image reconstruction of cerebral ischemia in a Wistar rat. **(a–f)** The images show coronal cross-sections of changes in oxy-, deoxy- and total hemoglobin through the rat brain midway between the lambda and bregma sutures (see line labeled 'cut' in **(g)**). The cross-sections were obtained by inducing unilateral carotid artery occlusions on the left side (a–c) and right side (d–f). An SSD system was used to measure the transmitted light intensities with four sources (white circles in (g)) and 12 detectors (black circles in (g)) placed on the top of the shaven rat head. Clearly visible are the lateral effects on the three hemodynamic parameters. (For more details see [11••].)

by Corlu *et al*. [54••] and Li *et al*. [55••] have shown that instead of performing μ_a reconstruction first, the multiple wavelength information can be used to calculate chromophore concentration directly. They showed that these new codes are much more stable and converge much faster to a correct result.

An example of a cerebral ischemia study in small animals is shown in Figure 4. Here, the previously described DYNOT imaging system was used in combination with a three-dimensional diffusion-theory-based MOBIIR scheme (Figure 2) to look at the effects of unilateral carotid occlusion in rodents [11••,12••]. Another SSD device was used by Culver *et al*. [13•] to establish the usefulness of DOT for studying stroke physiology. They occluded the middle cerebral artery in Sprague–Dawly rats and generated tomographic maps of relative cerebral blood volume changes, oxygen saturation, metabolic rate and oxygen consumption.

Functional stimulation studies were recently performed by Siegel *et al*. [32•]. Employing SSD data this group generated impressive maps of localized changes in cortical hemodynamics in response to forepaw stimulations and compared results with functional MRI data. They derived values for oxy-, deoxy- and total hemoglobin concentrations, using an algorithm that was based on the diffusion theory for semi-infinite media. In another study the same group also performed volumetric reconstructions [56]. In addition to SSD systems, FD methods were also employed to study hemodynamic responses to forepaw stimulation [28•]. The importance of proper source and detector placement was recently shown in a theoretical paper by Deghani and colleagues [57].

Imaging with exogenous contrast
Contrast mechanisms
In addition to endogenous contrast mechanisms that are used in blood oximetry studies, exogenous chromophores can also be employed for tomographic imaging. In general, one can distinguish between two different types of exogeneous contrast agents that lead to similar, yet different, imaging problems. The first class of probes con-

sists of bioluminescent markers [58•]. These markers emit light when they encounter certain biomolecular environments inside the animal [17,59] and the energy for this radiation is drawn directly from the local biochemical processes. The best-known examples for this type of effect are fireflies, which emit visible radiation upon release of luciferase into certain parts of their body [60].

The second class of probes is formed by fluorescent markers [29,44•,61]. Fluorescent markers, unlike bioluminescent markers, require an external excitation source to emit radiation. The light from this external source is absorbed by the fluorophore and re-emitted at a longer wavelength. Examples of frequently used fluorophores are indocyanine green, green and red fluorescence proteins [62], peptide-fluorescent dye conjugates that target specific cellular receptors [63], and enzyme-activatable fluorescence probes [64].

Fluorescence and bioluminescence imaging system

With some minor modifications, all of the systems described for endogenous systems can also be used for bioluminescence or fluorescence tomographic imaging. Bioluminescence systems can be thought of as SSD systems without an external light source. Fluorescence systems require the detection of the transmitted light intensities at the excitation and emission wavelength. Therefore, these systems involve either more detectors that are sensitive at these different wavelengths or two set of measurements during which wavelength-dependent filters are used to distinguish between the two wavelengths. Fluorescence measurements can be performed in all three domains (SSD, FD and TD), whereas bioluminescence is limited to SSD.

To apply MOBIIR schemes in fluorescence systems, two equation are necessary: one for the excitation wavelength and one for the emission wavelength [65••,66•]. These two equations are coupled through the source term of the emission wavelength, which depends on the solution of the equation of the excitation wavelength. The source term for the excitation wavelength is given by the known location of the optical fibers on the skin of the animal. The source term of the emission wavelength equation is itself an unknown, as location and concentration of the fluorescent marker that forms the sources are sought as part of the reconstruction process. Almost all codes currently available employ the diffusion equation, but first transport-theory-based codes have emerged [43••,67•].

Bioluminescence tomography (BLT) is basically the fluorescence problem without the excitation term. The source position and strength inside the medium are sought in a similar manner to SPECT; however, BLT is even more ill-posed than SPECT imaging, as light is strongly scattered. Therefore, BLT remains the most

challenging of all optical tomographic imaging systems, and the first publications to investigate this problem have only recently appeared [68,69•].

Comparison of different systems

Although fluorescence imaging is experimentally and computationally somewhat more involved, it offers several distinct advantages over bioluminescence imaging. First, fluorescence probes generate a much stronger signal than bioluminescence probes and yield a higher signal-to-noise ratio. Therefore, fluorescence imaging systems require much less sensitive (and therefore less expensive) detectors than bioluminescence imaging systems. Furthermore, many fluorophores emit light in the near-infrared wavelength range, which allows for deeper penetration into biological tissue. Most bioluminescent probes emit light at a shorter wavelength, where tissue is more absorbing and can therefore only be used for superficial lesion. In addition, the image reconstruction problem in bioluminescent imaging is much more ill-posed than in fluorescence imaging, which severely limits the achievable resolution. No BLT code has yet been presented, whereas first fluorescence tomographic imaging algorithms do exist and have shown promising results in small-animal imaging [46•,70–74,75••]. Of special importance here is the first non-contact tomographic imaging system developed by Schulz and coworkers [76••,77••].

Furthermore, as already mentioned, unlike BLT fluorescence imaging can be performed in the time or frequency domain. In this way, more information can be obtained about the fluorescent sources and the scattering and absorption properties of the background medium. Employing FD or TD techniques, fluorescence imaging also offers the possibility of obtaining spatial lifetime maps of fluorophore distribution inside tissues [78,79]. Fluorescence lifetime imaging could be used to analyse the local biochemical environment of a fluorophore, such as pH or oxygen levels or calcium ion concentrations [78,80]. These types of study are already widely performed in the fluorescence microscopy of single cells or tissue slices and could potentially be translated into fluorescence tomography for whole-body imaging of small animals. The only drawback of fluorescence imaging is that the tissue intrinsic auto-fluorescence is often higher than auto-bioluminescence; this can lead to increased noise.

Applications

There has been a great number of studies on inanimate tissue phantoms that mimic tissue anatomy and physiology. These studies have demonstrated that one can use optical tomography to reconstruct the spatial distribution of fluorophore concentrations and lifetimes from SSD-type measurements [46•,75••,76••,77••], as well as from FD systems [44•,65••,66•,70,81,82] and using TD methods [83]. *In vivo* studies that employ tomographic

Figure 5
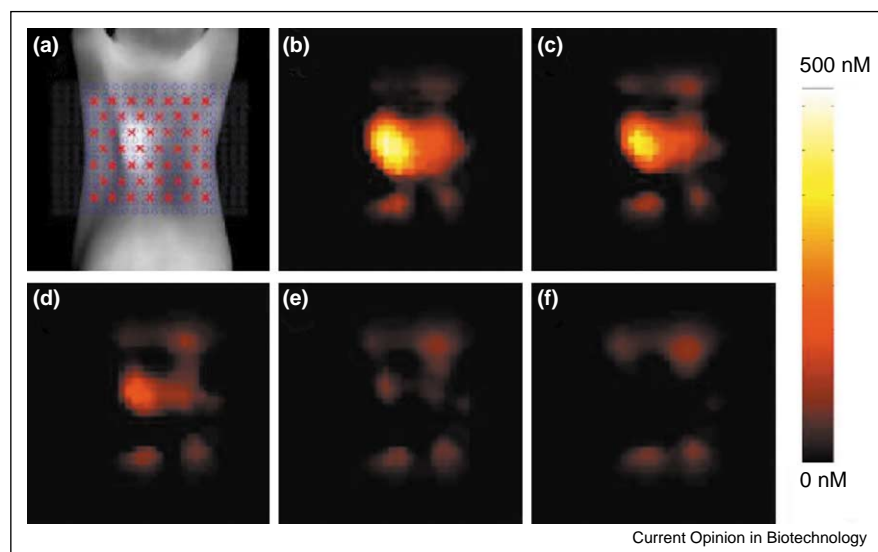
The figure shows the first *in vivo* transport-theory-based, three-dimensional, tomographic reconstruction results for fluorescence molecular imaging. The transport-theory-based model is particularly well suited to take small geometries and small source-detector separations into account, as they are encountered in small animals. The animal was injected with a Cy5.5-based fluorescent probe with high sensitivity to cathepsins produced in a Lewis lung carcinoma implanted in the left lung of the animal. For data acquisition the mouse was immersed into an imaging chamber containing a scattering matching fluid. One side of the chamber was illuminated with light (wavelength = 674 nm) emerging from 46 fibers arranged in a symmetric pattern (red crosses in (a)). A CCD camera captured the excitation and fluorescence light (wavelength = 694 nm) on the side opposite to the illuminating fibers (blue circles in (a)). The measured light intensities became input to the image reconstruction algorithm. **(a)** Shows the direct fluorescence image obtained with the CCD camera. The lung tumor can be seen as bright spot on the left-hand side. **(b–f)** Tomographic images of the fluorophore concentration at different depths: (b) 1 mm, (c) 2 mm, (d) 3 mm, (e) 4 mm and (f) 5 mm.

techniques have only just begun and mainly focus on cancer research. For example, it was shown that cathepsin B activity in 9L gliosarcomas implanted into one brain hemisphere of nude mice could be imaged using a cathepsin-B-sensitive molecular beacon (an enzyme-activatable fluorochome) [84,85••]. For this study the animals were immersed into a cylinder filled with matching fluid. The cylinder was surrounded by 24 source fibers and 36 detector fibers. The system was operated in SSD mode using 672 nm excitation light and detecting emissions at 710 nm ± 10 nm. In other studies, subcutaneously implanted HT1080 fibrosarcomas [86] and Lewis lung carcinomas [14] where imaged also using enzyme-activatable fluorescent probes. In both cases animals were immersed–in a rectangular container and transmission measurements performed using a CCD (charge-coupled device) camera. Figure 5 shows an example where a novel transport-theory-based code [43••,87] was used to produce a three-dimensional image of a lung carcinoma. Recently, Chen *et al*. [88] demonstrated the feasibility of tomographic detection of 2-cm-deep subsurface tumors in mice with a localization accuracy of 2–3 mm, using an FD system. Going beyond proof-of-principle studies, first fluorescence tomographic studies have started to emerge that show tumor response to chemotherapy [15••].

In vivo bioluminescence studies are currently limited to two-dimensional surface imaging of small animals [58•]. First studies have emerged that suggest the possibility of BLT imaging [68,69•]; however, these algorithms have only been applied to tissue phantoms and further validation studies in small animals need to be performed.

Conclusions

DOT is developing into a viable addition to currently existing biomedical imaging modalities, such as ultrasound, X-ray computed tomography, MRI, PET and SPECT. This novel imaging technique uses visible and near-infrared light ($\sim$500 nm $< \lambda <$ 900 nm) to probe the absorption and scattering properties of tissues. Recent technological and computational advances have led to first small-animal imaging systems, which are currently used to study cerebral ischemia and hemodynamics. The use of exogenous fluorescence and bioluminescence markers in optical tomography appears particularly promising in studying the molecular origins of cancer.

Future advances can be anticipated in the development of more accurate image reconstruction algorithms that use better models of light propagation in small animals, as well as hardware advances that will allow non-contact optical tomographic imaging. Finally, it can be expected

that the application of DOT will grow to include studies of cardiac diseases, arthritis and Alzheimer's, to name just a few.

References and recommended reading
Papers of particular interest, published within the annual period of review, have been highlighted as:

- of special interest
- of outstanding interest

1. Chance B, Alfano RR, Tromberg BJ, Tamura M, Eva M, Sevick-Muraca EM: *Optical tomography and spectroscopy of tissue V, Proceedings 4955*. SPIE-The International Society for Optical Engineering, Bellingham, WA; 2003.

2. *Biomedical Topical Meetings 2002 TOPS*, Volume 71. Edited by AA Sawchuk. Optical Society of America: Washington, DC; 2002.

3. Tuan Vo-Dinh: *Biomedical Photonics Handbook*. Boca Raton, FL: CRC Press LLC; 2003.

4. Pogue BW, Poplack SP, McBride TO, Wells WA, Osterman KS, Osterberg UL, Paulsen KD: **Quantitative hemoglobin tomography with diffuse near-infrared spectroscopy: pilot results in the breast**. *Radiology* 2001, **218**:261-266.

5. Ntziachristos V, Yodh AG, Schnall MD, Chance B: **MRI-guided diffuse optical spectroscopy of malignant and benign breast lesions**. *Neoplasia* 2002, **4**:347-354.

6. Hielscher AH, Klose AD, Scheel AK, Moa-Anderson B, Backhaus M, Netz U, Beuthan J: **Sagittal laser optical tomography for imaging of rheumatoid finger joints**. *Phys Med Biol* 2004, **49**:1147-1163.

7. Scheel AK, Backhaus M, Klose AD, Moa-Anderson B, Netz U, Hermann KG, Beuthan J, Müller GA, Burmester GR, Hielscher AH: **First clinical evaluation of sagittal laser optical tomography for detection of synovitis in arthritic finger joints**. *Ann Rheum Dis* 2005, **64**:239-245.

8. Hillman EMC, Hebden JC, Schweiger M, Dehghani H, Schmidt FEW, Delpy DT, Arridge SR: **Time resolved optical tomography of the human forearm**. *Phys Med Biol* 2001, **46**:1117-1130.

9. Benaron DA, Hintz SR, Villringer A, Boas D, Kleinschmitt A, Frahm J, Hirth C, Obrig H, van Houten JC, Kermit EL *et al.*: **Noninvasive functional imaging of brain using light**. *J Cereb Blood Flow Metab* 2000, **20**:469-477.

10. Bluestone AY, Abdoulaev G, Schmitz C, Barbour R, Hielscher A: **Three-dimensional optical-tomography of hemodynamics in the human head**. *Opt Express* 2001, **9**:272-286.

11. Bluestone AY, Stewart M, Lei B, Kass IS, Lasker J, Abdoulaev GS,
•• Hielscher AH: **Three-dimensional optical tomographic brain imaging in small animals, part I: hypercapnia**. *J Biomed Opt* 2004, **9**:1046-1062.
First use of a model-based image reconstruction scheme that incorporates irregularly shaped boundaries of rat head, as well as *a priori* anatomical knowledge of rat brain. A comprehensive code validation is performed.

12. Bluestone AY, Stewart M, Lasker J, Abdoulaev GS, Hielscher AH:
•• **Three-dimensional optical tomographic brain imaging in small animals, part II: unilateral carotid occlusion**. *J Biomed Opt* 2004, **9**:1063-1073.
See the annotation for [11••].

13. Culver JP, Durduran T, Furuya D, Cheung C, Greenberg JH,
• Yodh AG: **Diffuse optical tomography of cerebral blood flow,**
oxygenation, and metabolism in rat during focal ischemia.
J Cereb Blood Flow Metab 2003, **23**:911-924.
First study to demonstrate the feasibility of optical tomographic imaging of stroke in small animals.

14. Graves EE, Weissleder R, Ntziachristos V: **Fluorescence molecular imaging of small animal tumor models**. *Curr Mol Med* 2004, **4**:419-430.

15. Ntziachristos V, Schellenberger EA, Ripoll J, Yessayan D,
•• Graves E, Bodganov A, Josephson L, Weissleder R: **Visualization of antitumor treatment by means of fluorescence molecular tomography with an annexin V-Cy5.5 conjugate**. *Proc Natl Acad Sci USA* 2004, **101**:12294-12299.
First paper to go beyond proof-of-principle and code validation to apply optical tomographic methods to study the effects of an antitumor drug.

16. Weissleder R, Mahmood U: **Molecular imaging**. *Radiology* 2001, **219**:316-333.

17. Contag PR: **Whole-animal cellular and molecular imaging to accelerate drug development**. *Drug Discov Today* 2002, **7**:555-562.

18. Bornhop DJ, Contag CH, Licha K, Murphy CJ: **Advances in contrast agents, reporters, and detection**. *J Biomed Opt* 2001, **6**:106-110.

19. Welch AJ, van Gemert MJC: *Optical-Thermal Response of Laser-Irradiated Tissue*. New York: Plenum; 1995.

20. Mourant JR, Canpolat M, Brocker C, Esponda-Ramos O, Johnson TM, Matanock A, Stetter K, Freyer JP: **Light scattering from cells: the contribution of the nucleus and the effects of proliferative status**. *J Biomed Opt* 2000, **5**:131-137.

21. Mourant JR, Freyer JP, Hielscher AH, Eick AA, Shen D, Johnson TM: **Mechanisms of light scattering from biological cells relevant to noninvasive optical-tissue diagnostics**. *Appl Opt* 1998, **37**:3586-3593.

22. Hebden JC, Arridge SR, Delpy DT: **Optical imaging in medicine.1. Experimental techniques**. *Phys Med Biol* 1997, **42**:825-840.

23. Patterson MS, Chance B, Wilson BC: **Time resolved reflectance and transmittance for the noninvasive measurement of tissue optical properties**. *Appl Opt* 1989, **28**:2231-2336.

24. Turner GM, Zacharakis G, Ripoll J, Ntziachristos V: **Early photon
• tomographic imaging with 360-degree sample rotation**.
In *Proceedings of the Biomedical Optics Topical Meeting, April 14–17, 2004, Miami Beach, FL*. Optical Society of America, Washington, DC; Abstract # WF23.
Only report to date of a small-animal tomography system that used TD instrumentation.

25. Tu T, Chen Y, Zhang J, Intes X, Chance B: **Analysis on performance and optimization of frequency-domain near-infrared instruments**. *J Biomed Opt* 2002, **7**:643-649.

26. Pham TH, Coquoz O, Fishkin JB, Anderson E, Tromberg BJ: **Broad bandwidth frequency domain instrument for quantitative tissue optical spectroscopy**. *Rev Sci Instrum* 2000, **71**:2500-2513.

27. Cheung C, Culver JP, Takahashi K, Greenberg JH, Yodh AG: *In vivo* **cerebrovascular measurement combining diffuse near-infrared absorption and correlation spectroscopies**. *Phys Med Biol* 2001, **46**:2053-2065.

28. Yu G, Durduran T, Furuya D, Greenberg JH, Yodh AG: **Frequency-
• domain multiplexing system for *in vivo* diffuse light measurements of rapid cerebral hemodynamics**.
Appl Opt 2003, **42**:2931-2939.
Introduces the most advanced FD system for small-animal oximetry to date.

29. Thompson AB, Sevick-Muraca EM: **Near-infrared fluorescence contrast-enhanced imaging with intensified charge-coupled device homodyne detection: measurement precision and accuracy**. *J Biomed Opt* 2003, **8**:111-120.

30. Schmitz CH, Löcker M, Lasker JM, Hielscher AH, Barbour RL:
• **Instrumentation for fast functional optical tomography**.
Rev Sci Instrum 2002, **73**:429-439.

Reports on a tomographic imaging system with the highest data acquisition rate currently available. This system, called DYNOT, is one of the first commercially available instruments.

31. Siegel AM, Marota JJA, Boas DA: **Design and evaluation of a continuous-wave diffuse optical tomography system**. *Opt Express* 1999, **4**:287-298.

32. Siegel AM, Culver JP, Madeville JB, Boas DA: **Temporal**
• **comparison of functional brain imaging with diffuse optical tomography and fMRI during rat forepaw stimulation**. *Phys Med Biol* 2003, **48**:1391-1403.
The first publication to compare results obtained from optical tomography with MRI data.

33. Hielscher AH, Klose AD, Hanson KM: **Gradient-based iterative image reconstruction scheme for time-resolved optical tomography**. *IEEE Trans Med Imaging* 1999, **18**:262-271.

34. Arridge SR: **Optical tomography in medical imaging**. *Inverse Problems* 1999, **15**:R41-R93.

35. Klose AK, Hielscher AH: **Quasi-Newton methods in optical tomographic imaging**. *Inverse Problems* 2003, **19**:387-409.

36. Hielscher AH, Bartel S: **Use of penalty terms in gradient-based iterative reconstruction schemes for optical tomography**. *J Biomed Opt* 2001, **6**:183-192.

37. Roy R, Sevick-Muraca EM: **Three-dimensional unconstrained and constrained image-reconstruction techniques applied to fluorescence, frequency-domain photon migration**. *Appl Opt* 2001, **40**:2206-2215.

38. Brooksby BA, Dehghani H, Pogue BW, Paulsen KD: **Near-infrared (NIR) tomography breast image reconstruction with *a priori* structural information from MRI: algorithm development for reconstructing heterogeneities**. *IEEE Journal of Selected Topics in Quantum Electronics* 2003, **9**:199-209.

39. Hielscher AH, Alcouffe RE, Barbour RL: **Comparison of finite-difference transport and diffusion calculations for photon migration in homogeneous and heterogeneous tissue**. *Phys Med Biol* 1998, **43**:1285-1302.

40. Klose AD, Netz U, Beuthan J, Hielscher AH: **Optical tomography**
•• **using the time-independent equation of radiative transfer, Part 1: forward model**. *J Quant Spectr Radiat Transf* 2002, **72**:691-713.
Provides a comprehensive assessment of a MOBIIR code that is based on the equation radiative transfer. Besides detailed testing of forward and inverse algorithms, the authors present an excellent introduction to adjoint differentiation.

41. Klose AD, Hielscher AH: **Optical tomography using the**
•• **time-independent equation of radiative transfer. Part 2: inverse model**. *J Quant Spectr Radiat Transf* 2002, **72**:715-732.
See the annotation for [40••].

42. Abdoulaev G, Hielscher AH: **Three-dimensional optical tomography with the equation of radiative transfer**. *J Electron Imaging* 2003, **12**:560-594.

43. Klose AK, Ntziachristos V, Hielscher AH: **The inverse source**
•• **problem based on the radiative transfer equation in molecular optical imaging**. *J Comput Phys* 2005, **202**:323-345.
First comprehensive publication on how to use the equation of radiative transfer in fluoresence small-animal imaging.

44. Sevick-Muraca EM, Houston JP, Gurfinkel M: **Fluorescence-**
• **enhanced, near infrared diagnostic imaging with contrast agents**. *Curr Opin Chem Biol* 2002, **6**:642-650.
Excellent short review of recent advances in fluorescence imaging.

45. Pei Y, Graber HL, Barbour RL: **Influence of systematic errors in reference states on image quality and on stability of derived information for DC optical imaging**. *Appl Opt* 2001, **40**:5576-5755.

46. Ntziachristos V, Weissleder R: **Experimental three-dimensional**
• **fluorescence reconstruction of diffuse media by use of a normalized Born approximation**. *Opt Lett* 2001, **26**:893.
This paper provides a convincing case on how quantitative fluorescence tomography is possible by dividing the emission measurements by the excitation measurements. In this way the authors overcome common calibration problems in optical tomography.

47. Arridge SR, Lionheart WRB: **Nonuniqueness in diffusion-based optical tomography**. *Opt Lett* 1998, **23**:882-884.

48. Houston JP, Thompson AB, Gurfinkel M, Sevick-Muraca EM: **Sensitivity and depth penetration of continous wave versus frequency-domain photon migration near-infrared fluorescence contrast enhanced imaging**. *Photochem Photobiol* 2003, **77**:420-430.

49. Pei YL, Graber HL, Barbour RL: **Normalized-constraint algorithm for minimizing inter-parameter crosstalk in DC optical tomography**. *Opt Express* 2001, **9**:97-109.

50. Xu Y, Gu XJ, Khan T, Jiang HB: **Absorption and scattering images of heterogeneous scattering media can be simultaneously reconstructed by use of DC data**. *Appl Opt* 2002, **41**:5427-5437.

51. Hielscher AH, Bluestone AY, Abdoulaev GS, Klose AD, Lasker J,
•• Stewart M, Netz U, Beuthan J: **Near-infrared diffuse optical tomography**. *Dis Markers* 2002, **18**:313-337.
Provides a detailed overview of optical tomographic imaging for breast, brain and small-animal imaging.

52. Cheng X, Boas BA: **Systematic diffuse optical image errors resulting from uncertainty in the background optical properties**. *Optics Express* 1999, **4**:299-307.

53. Wray S, Cope M, Delpy DT: **Characteristics of the near infrared absorption spectra of cytochrome aa_3 and hemoglobin for the noninvasive monitoring of cerebral oxygenation**. *Biochim Biophys Acta* 1988, **933**:184-192.

54. Corlu A, Durduran T, Choe R, Schweiger M, Hillman EMC,
•• Arridge SR, Yodh AG: **Uniqueness and wavelength optimization in continuous-wave multispectral diffuse optical tomography**. *Opt Lett* 2003, **28**:2339-2341.
Together with [55••], these papers introduce one of the most interesting recent advances in optical tomographic imaging. The authors show how measurements at multiple wavelengths can be used to directly calculate chromophore concentrations and at the same time reduce the ill-posedness in optical tomographic imaging.

55. Li A, Zhang Q, Culver JP, Miller EL, Boas DA: **Reconstructing**
•• **chromosphere concentration images directly by continuous-wave diffuse optical tomography**. *Opt Lett* 2004, **29**:256-258.
See the annotation for [54••].

56. Culver JP, Siegel AM, Stott JJ, Boas DA: **Volumetric diffuse optical tomography of brain activity**. *Opt Lett* 2003, **28**:2061-2063.

57. Xu H, Dehghani H, Pogue BW, Springett R, Paulsen KD, Dunn JF: **Near-infrared imaging in the small animal brain: optimization of fiber positions**. *J Biomed Opt* 2003, **8**:102-110.

58. Contag CH, Ross BD: **It's not just about anatomy: *in vivo***
• **bioluminescence imaging as an eyepiece into biology**. *J Magn Reson Imaging* 2002, **16**:378-387.
Excellent introduction to bioluminescence imaging, even though tomographic imaging is not discussed much. Bioluminescence tomography is still in nascent stage.

59. Rice BW, Cable MD, Nelson MB: ***In vivo* imaging of light-emitting probes**. *J Biomed Opt* 2001, **6**:432-440.

60. Bhaumik S, Gambhir S: **Optical imaging of renilla luciferase reporter gene expression in living mice**. *Proc Natl Acad Sci USA* 2002, **99**:377-382.

61. Gillies RJ: ***In vivo* molecular imaging**. *J Cell Biochem* 2002, (**Supplement 39**):231-238.

62. Mathieu S, El-Battari A: **Monitoring E-selectin-mediated adhesion using green and red fluorescent proteins**. *J Immunol Methods* 2003, **272**:81-92.

63. Becker A, Hessenius C, Licha K, Ebert B, Sukowski U, Semmler W, Wiedenman B, Grotzinger C: **Receptor-targeted optical imaging of tumors with near infrared fluorescent ligands**. *Nat Biotechnol* 2001, **19**:327-331.

64. Bremer C, Tung C, Weissleder R: **Imaging of metalloproteinase 2 inhibition *in vivo***. *Nat Med* 2001, **7**:743-748.

65. Milstein AB, Oh S, Webb KJ, Bouman CA, Zhang Q, Boas DA,
•• Millane RP: **Fluoresence optical diffusion tomography**.
Appl Opt 2003, **42**:3081-3094.
A very thorough paper on theoretical approaches to model-based itera-
tive image reconstructions in fluorescence tomography.

66. Eppstein MJ, Hawrysz DJ, Godavarty A, Sevick-Muraca EM:
• **Three-dimensional Bayesian image reconstruction from
sparse noisy data sets: near-infrared fluorescence
tomography**. *Proc Natl Acad Sci USA* 2002, **99**:9619-9624.
This paper provides an excellent introduction to Bayesian methods in
fluorescence tomographic imaging.

67. Klose AD, Hielscher AH: **Fluorescence tomography with
• simulated data based on the equation of radiative transfer**.
Opt Lett 2003, **28**:1019-1021.
The first paper to report on a fluorescence tomography algorithm that is
not based on the diffusion approximation to the equation of radiative
transfer.

68. Wang G, Li Y, Jiang M: **Uniqueness in bioluminescence
tomography**. *Med Phys* 2004, **31**:2289-2299.

69. Gu X, Zhang Q, Larcom L, Jiang H: **Three-dimensional
• bioluminescence tomography with model-based
reconstruction**. *Opt Express* 2004, **20**:3996-4000.
The only paper to date to show tomographic reconstruction results for
bioluminescence probes.

70. Lee J, Sevick-Muraca EM: **Three-dimensional fluorescence
enhanced optical tomography using referenced frequency-
domain photon migration measurements at emission and
excitation wavelengths**. *J Opt Soc Am A* 2002, **19**:759-771.

71. Roy R, Sevick-Muraca EM: **A numerical study of gradient-based
nonlinear optimization methods for contrast enhanced optical
tomography**. *Opt Exp* 2001, **9**:49.

72. Chang J, Graber HL, Barbour RL: **Imaging of fluorescence in
highly scattering media**. *IEEE Trans Biomed Eng* 1997,
44:810-822.

73. Chang J, Graber HL, Barbour RL: **Luminescence optical
tomography of dense scattering media**. *J Opt Soc Am A* 1997,
14:288-299.

74. Lee J, Sevick-Muraca EM: **Fluorescence-enhanced absorption
imaging using frequency-domain photon migration: tolerance
to measurement error**. *J Biomed Opt* 2001, **6**:58-67.

75. Ntziachristos V, Weissleder R: **Charge-coupled-device based
•• scanner for tomography of fluorescent near-infrared probes in
turbid media**. *Med Phys* 2002, **29**:803-809.
Describes one of the best functional systems for small-animal fluores-
cence tomography.

76. Schulz RB, Ripoll J, Ntziachristos V: **Noncontact optical
•• tomography of turbid media**. *Opt Lett* 2003, **28**:1701-1703.
One of the most exciting developments in recent years is the non-contact
approach to optical tomography. This paper and [77••] describe the

theory and first experimental results in this area and set the standards
for future developments.

77. Schulz RB, Ripoll J, Ntziachristos V: **Experimental fluorescence
•• tomography of tissue with noncontact measurements**.
IEEE Trans Med Imaging 2004, **23**:492-500.
See the annotation for [76••].

78. Paithankar DY, Chen AU, Pogue BW, Patterson MS,
Sevick-Muraca EM: **Imaging of fluorescent yield and lifetime
from multiply scattered light reemitted from random media**.
Appl Opt 1997, **36**:2260-2272.

79. O'Leary MA, Boas DA, Li XD, Chance B, Yodh AG: **Fluorescence
lifetime imaging in turbid media**. *Opt Lett* 1996, **21**:158.

80. Shives E, Xu Y, Jiang HB: **Fluorescence lifetime tomography
of turbid media based on an oxygen-sensitive dye**. *Opt Express*
2002, **10**:1557-1562.

81. Roy R, Godavarty A, Sevick-Muraca EM: **Fluorescence-
enhanced optical tomography using referenced
measurements of heterogeneous media**. *IEEE Trans Med
Imaging* 2003, **22**:824-836.

82. Milstein AB, Stott JJ, Oh S, Boas DA, Millane RP, Bouman CA,
Webb KJ: **Fluorescence optical diffusion tomography
using multiple-frequency data**. *J Opt Soc Am A* 2004,
21:1035-1059.

83. Haiyong Quan, Zhixiong Guo: **Fast 3-D optical imaging
with transient fluorescence signals**. *Opt Express* 2004,
12:449-457.

84. Ntziachristos V, Tung CH, Bremer C, Weissleder R: **Fluorescence
molecular tomography resolves protease activity *in vivo***.
Nat Med 2002, **8**:757-760.

85. Ntziachristos V, Bremer C, Weissleder R: **Fluorescence imaging
•• with near-infrared light: new technological advances that
enable *in vivo* molecular imaging**. *Eur Radiol* 2003, **13**:195-208.
Best review in the field of optical fluorescence tomography. A must read
for everybody who enters the field.

86. Graves EE, Ripoll J, Weissleder R, Ntziachristos V: **A
submillimeter resolution fluorescence molecular imaging
system for small animal imaging**. *Med Phys* 2003, **30**:901-911.

87. Klose AD, Ntziachristos V, Hielscher AH: ***In vivo* fluorescence
molecular imaging with a radiative transfer model**. *Mol Imaging*
2004, **3**:230.

88. Chen Y, Zheng G, Zhang ZH, Blessington D, Zhang M, Li H, Liu Q,
Zhou L, Intes X, Achilefu S, Chance B: **Metabolism-enhanced
tumor localization by fluorescence imaging: *in vivo* animal
studies**. *Opt Lett* 2003, **28**:2070-2072.

89. Ren K, Abdoulaev G, Bal G, Hielscher AH: **Algorithm for solving
the equation of radiative transfer in the frequency domain**.
Optics Letts 2004, **29**:578-580.